Plasticity: Adiabatic Shear Localization

Shear localization occurs when plastic deformation localizes on a thin region of a specimen. It is very important because it is often a precursor to failure. In most cases, shear localization is associated with a local softening of the structure. This softening can be due to thermal or geometrical reasons. In geometrical softening, the structure orients itself to a direction that is easier (i.e., requires less stress) for glide. The rotation of crystallographic slip planes in response to straining in ductile crystalline solids is an example. However, shear localization is not restricted to crystalline solids; metallic glasses and partially crystalline polymers are very prone to shear localization. Granular and fragmented ceramics and rocks undergo localization. For these cases, thermal softening is replaced by structural softening, such as particle breakdown. In special cases, localization has been predicted to occur even during hardening (Rudnicki and Rice 1975). In thermal softening, the local increase in temperature can result in a softening that leads to localization. In the extreme case when the strain rate is so high that the local heat generated cannot escape from the deformation area, these bands are called *adiabatic shear bands*. Regardless of the initial softening mechanism, the localized deformation leads to an acceleration of strain rate. Eventually, there are heat concentration and thermal effects in most situations. There are several excellent reviews available in the literature. Review articles by Rogers (1979), Stelly and Dormeval (1986), and the proceedings of a 1992 symposium on shear instabilities (Armstrong *et al.* 1994) contain a significant amount of information. The reader is also referred to the book by Meyers (1994) which contains a chapter on the subject. In this article we will introduce the fundamental aspects and then focus on significant recent developments.

1. *Mechanical Modeling*

The simplest approaches to shear localization are mathematical expressions of the following statement: shear localization occurs when the effect of hardening due to plastic deformation and strain-rate hardening are overcome by softening due to heating. This was expressed first by Tresca in the late 1800s, rediscovered by Zener and Hollomon (1944) and mathematically developed by Recht (1964). If one expresses the shear stress, τ, as a function of shear strain, γ, shear strain rate, $\dot{\gamma}$, and temperature, T:

$$\tau = f(\gamma, \dot{\gamma}, T) \tag{1}$$

The Zener–Hollomon condition is:

$$\frac{d\tau}{d\gamma} = 0 \tag{2}$$

If it is applied to Eqn. (1):

$$\frac{d\tau}{d\gamma} = \left(\frac{\partial \tau}{\partial \gamma}\right)_{\dot{\gamma},T} + \left(\frac{\partial \tau}{\partial \dot{\gamma}}\right)_{\gamma,T} \frac{d\dot{\gamma}}{d\gamma} + \left(\frac{\partial \tau}{\partial T}\right)_{\gamma,\dot{\gamma}} \frac{dT}{d\gamma} \tag{3}$$

Clifton (1979), Bai (1981), and Molinari and Clifton (1983) introduced analyses of shear instabilities that used the perturbation method together with the conservation equations. These analyses enable the prediction of the effect of perturbations on the onset of shear-band formation and provide a guideline to the prediction of the evolution of a shear band. Clifton (1979) improved the simplified criterion for instability proposed by Zener and Hollomon (1944) and Recht (1964), using an initial perturbation in temperature with wave number ξ,

$$\left[\frac{1}{\tau}\left(\frac{d\tau}{d\gamma}\right) + \frac{\alpha}{\rho C}\left(\frac{d\tau}{dT}\right)\right] m\dot{\gamma} + \frac{\lambda \xi^2}{\rho C} \neq 0 \tag{4}$$

m is the strain rate sensitivity, ρ the density, C the heat capacity, α the heat-to-work conversion factor, λ the heat conductivity. The expression derived by Bai (1968) is similar. Fressengeas and Molinari (1987) introduced a new perturbation method, called the relative perturbation method, which accounted for the nonsteadiness of plastic flow. Leroy and Molinari (1993) and Molinari and Le Roy (1993) extended the analysis of shear instabilities by using a two-dimensional bifurcation method. They obtained variation in shear along the band and a patterning behavior, suggestive of vorticity. This will be discussed again.

One-dimensional models of shear bands have the limitation that the shear strain is constant along the length of the band. This is not a true realistic representation of shear bands that exhibit a front, such as a Mode II or Mode III crack, and shear strains that vary along the length of the band. This aspect was analyzed by Kuriyama and Meyers (1986), who treated the shear band as having an extremity. They showed that the advance of a shear band proceeded by the softening of the material ahead of the tip of the band. Figure 1 shows the stress–strain curves considered to represent the adiabatic and isothermal responses. The adiabatic curve exhibits a maximum, whereas the isothermal curve (dashed) shows continuous hardening. The results are strikingly different at the tip of a notch that represents the extremity of the shear band. In the adiabatic case, a thin region of high strain forms ($\gamma \geqslant 0.0646$) and propagates while in the isothermal case, this region of strain concentration is much more modest. This computation shows the manner in which a shear band propagates. Grady (1994) developed a simplified two-dimensional model for the shear band, which contained a process zone. In analogy with fracture mechanics in which the crack tip

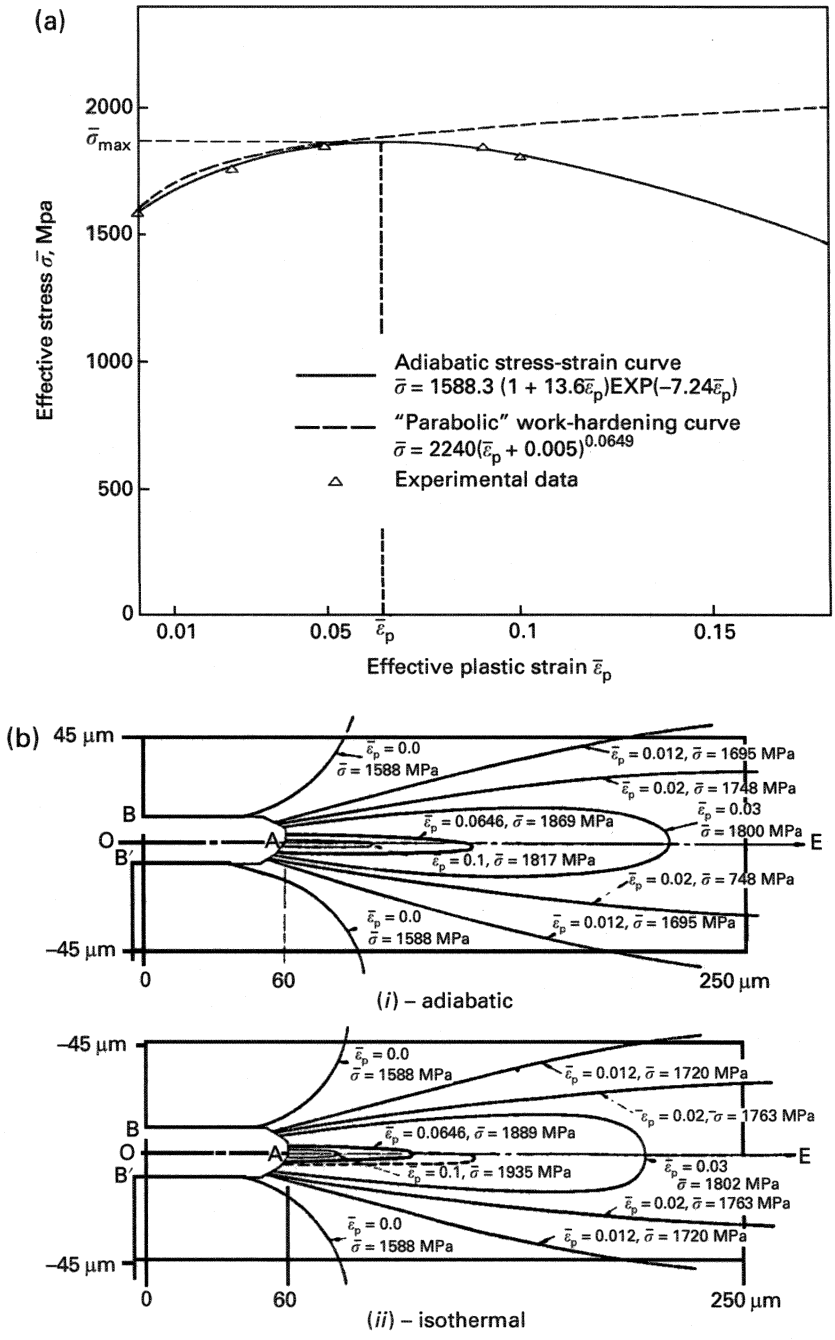

Figure 1
(a) Stress strain curves representing adiabatic (full line) and isothermal (dashed line) response of a HY-TUF steel in quenched and tempered condition (data from Olson *et al.* 1981), (b) plastic strain fields at the tip of a notch representing tip of band; (i) isothermal, (ii) adiabatic (after Kuriyama and Meyers 1986).

is the critical area for propagation, they developed an expression for the shear-band toughness, K_s, as:

$$K_s = \sqrt{2G\Gamma_s} \tag{5}$$

G is the elastic shear modulus and Γ_s is the shear-band dissipation energy. This shear-band dissipation energy varies over a wide range, from 15 kJ m^{-2} for uranium to 800 kJ m^{-2} for copper.

2. *Microstructural Aspects*

At the microstrutural level, the material is not a homogeneous continuum. The initiation of shear localization is a critical event, which can be triggered either by external, geometrical factors, or internal, microstructural factors. External initiation sites are regions of stress and strain concentration; microstructural sites are regions that undergo localized softening by some mechanism. Possible microstructural initiation sites are fractured second phase particles, dislocation pile-ups being released as an avalanche, geometrical softening resulting from the rotation of atomic planes towards orientations with a lower Schmid factor, and preferential slip paths produced by martensite transformation and twinning. The increase in Schmid factor of a grain with plastic deformation leads to localized softening which can initiate a shear band. The localized deformation of one grain can propagate along a band. This mechanism of localization through the cooperative plastic deformation of grains has been modeled by Peirce *et al.* (1984), and Anand and Kalidindi (1994). A dislocation pile-up, upon bursting through a grain boundary, can generate the local temperature rise and plastic deformation that would initiate shear band. This mechanism has been proposed by Armstrong *et al.* (1982), who performed calculations that indicate that the heat generated in a pile-up release is sufficient to initiate a shear band. Another very interesting mechanism was advanced by Weertman and Hecker (1983). They proposed that local dislocation reorganization produced elongated dislocation-free regions that were initial shear bands. Meyers *et al.* (1983) made observations of a similar nature on shock-loaded nickel subjected to subsequent tension. Localized regions (shaped like an oblate spheroid), virtually dislocation-free, were produced from the densely deformed material, leading to shear failure by a softening mechanism.

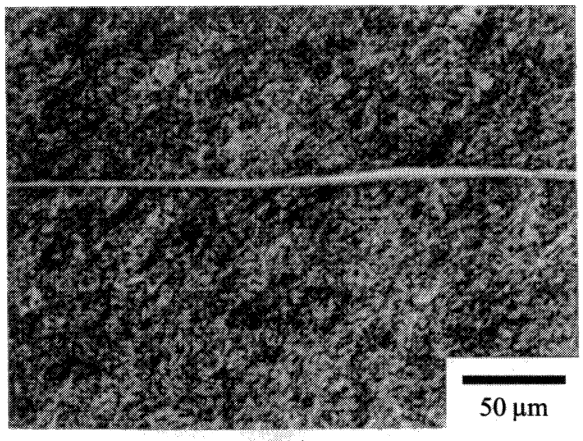

Figure 2
(a) Shear band in AISI 4340 quenched and tempered steel (from *Met. Trans.*, 1990, **21A**, 707), (b) Voids generated inside of shear band in Ti-6%Al-4%V alloy.

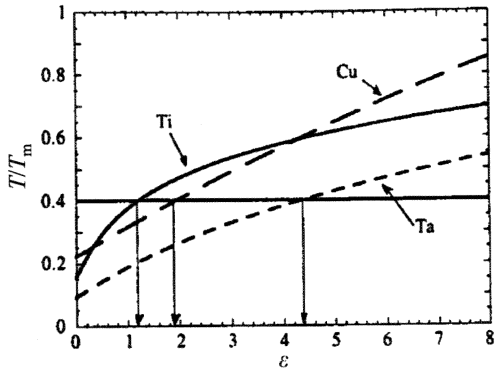

Figure 3
Calculated adiabatic temperature rises in Ta, Ti, and Cu.The line $T/T_m = 0.4$ marks the onset of dynamic recrystallization.

Figure 2(a) shows a typical shear band in quenched and tempered AISI 4340 steel. In different materials, the thickness and morphology vary somewhat. Nevertheless, the thickness is usually of the order of 10–200 μm; the shear strains inside the shear bands

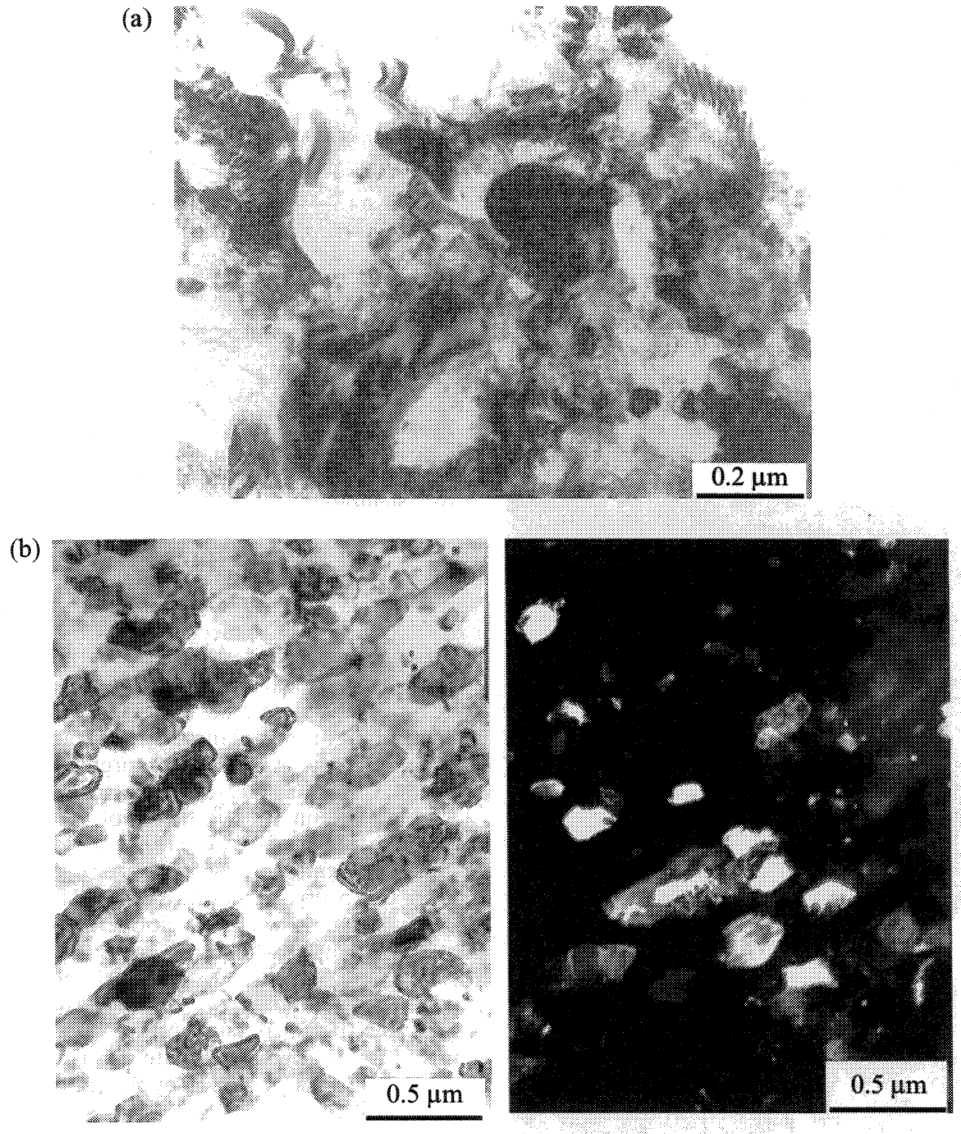

Figure 4
Submicrometer sized grains observed in shear bands, (a) titanium (from *Mech. Mater.*, 1994, **17**, 175), (b) Al–Li alloy).

reach extremely high values (of the order of 50 and higher). Adiabatic shear bands are the favorite sites for failure, either by ductile void nucleation, growth, and coalescence, or by cracking. The material within the shear band is heated to a high temperature and, therefore, has a lower flow stress than the surrounding matrix. Thus, tensile stresses will open voids at the shear band. Figure 2(b) shows a shear band that gave rise to voids; the void diameter is initially limited by the band thickness. Alternatively, after cooling, the material in the shear band can be harder and more brittle than the surrounding matrix. A number of examples of failure initiation at the shear bands are described by Grebe *et al.* (1985), Wittman *et al.* (1990), Meyers and Wittman (1990), and Xue *et al.* (1992).

The microstructural evolution inside the shear band has been actively studied from the mid-twentieth century, and different processes can occur:

- Dynamic recovery
- Dynamic recrystallization
- Phase transformation
- Strain-induced precipitate dissolution

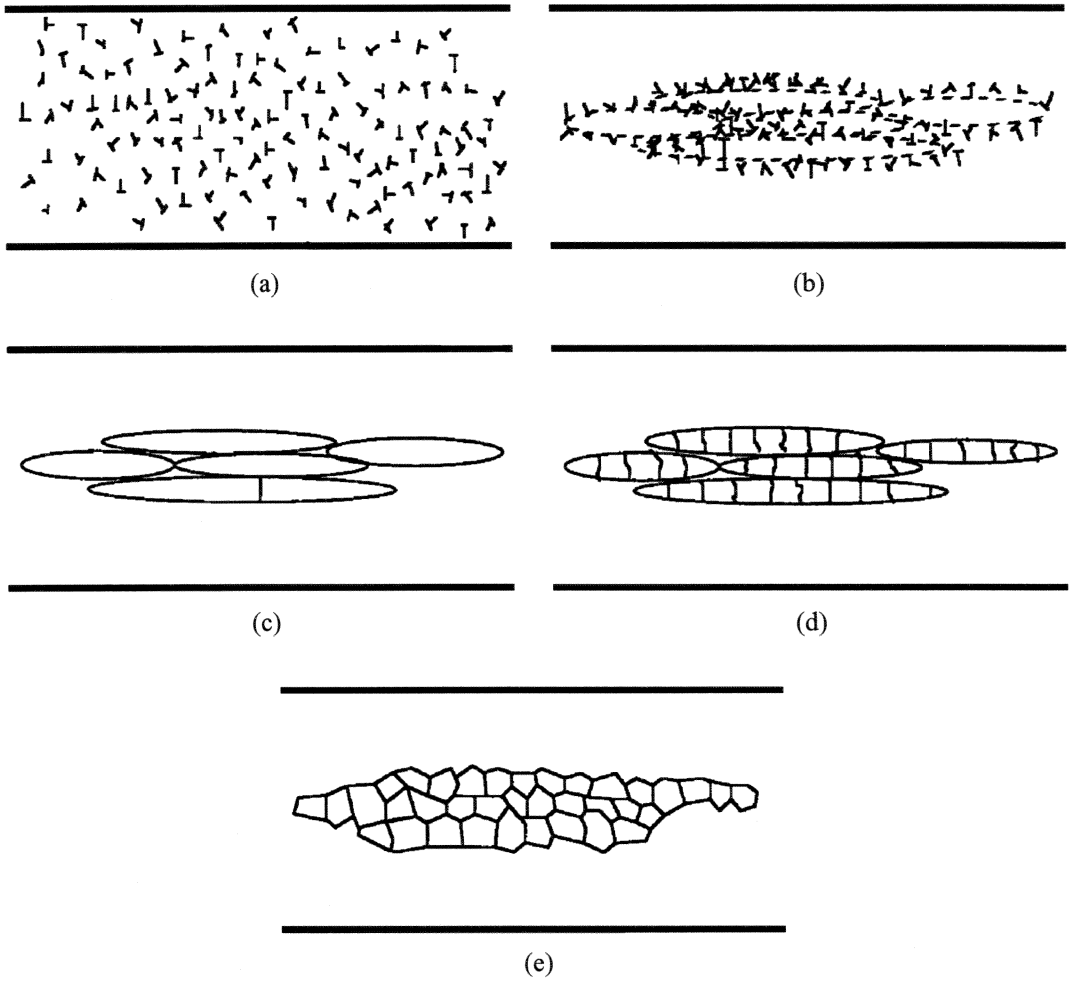

Figure 5
Schematic illustration of microstructural evolution during high strain-rate deformation. (a) Randomly distributed dislocations, (b) Elongated dislocation cell formation (i.e., dynamic recovery), (c) Elongated subgrain formation, (d) Initial break-up of elongated subgrains and (e) Recrystallized microstructure (from *Mater. Sci. Eng.*, 1997, **A229**, 23)

- Melting and resolidification
- Amorphization (by rapid quenching from the liquid)
- Crystallization (in metallic glasses)

These processes can occur concurrently or separately. It is often very difficult to establish whether the structures observed were produced during deformation or during post-deformation cooling. The older literature referred exclusively to *deformed* (or *deformation*) and *transformed* (or *transformation*) bands, but it is now recognized that the range of phenomena occurring in shear bands is much more complex.

It was independently discovered by Stelly and Dormeval (1986) and Grebe *et al.* (1985) for Ti-6%Al-4%V, and Meyers and Pak (1986) for titanium, that the structure inside the shear band consisted of fine (0.1–0.3 μm) recrystallized grains. The temperatures produced in the shear bands can reach very high values. Figure 3 shows calculated temperatures for three representative metals. The recrystallization temperature is usually taken as $0.4T_m$. This value is marked on the figure and it is seen that it is easily reached within shear bands, in which the shear strains can exceed 50. Figure 4 shows these recrystallized grains for titanium and an Al–Li alloy. A number of investigators have observed recrystallized structures inside shear bands. Of particular interest are armor steels, and Meunier *et al.* (1992) have found strikingly analogous results: the material within the shear band consisted of nanosize grains ($\sim$ 50–200 nm).

The importance of dynamic recrystallization in

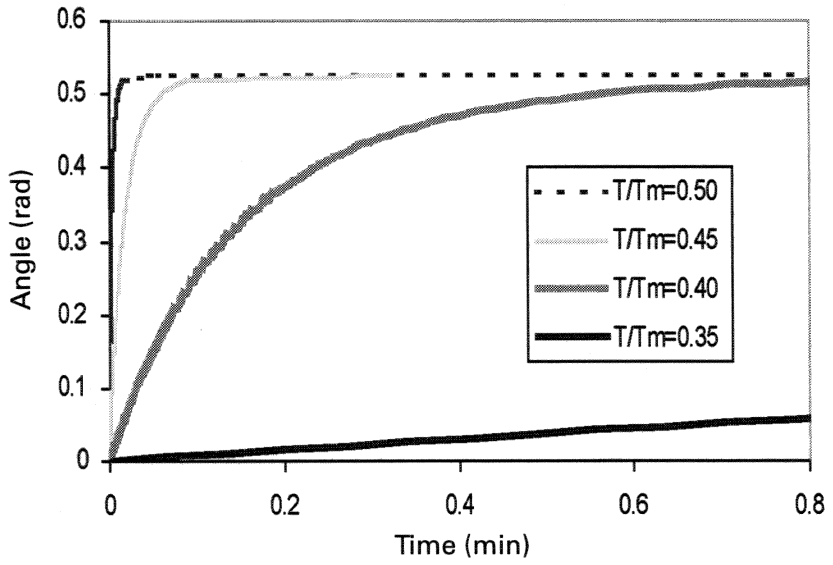

Figure 6
Rotation of grain boundaries for subgrain size of 0.1 μm in copper.

shear-band formation indicates that the critical event governing localization is the attainment of the recrystallization temperature. Derby (1991) classifies dynamic recrystallization mechanisms into rotational and migrational types. Dynamic recrystallization needs concurrent plastic deformation. Meyers and Pak (1986) suggested a rotational recrystallization mechanism in titanium, and this has been quantitatively developed. Figure 5 shows the primary features of the process by which rotational dynamic recrystallization is thought to occur. As can be seen from this figure, a homogeneous distribution of dislocations (Fig. 5(a)) rearranges itself into elongated dislocation cells (Fig. 5(b), dynamic recovery). As the deformation continues and as the misorientation increases, these cells become elongated subgrains (Fig. 5(c)).

Eventually, the elongated subgrains break up into approximately equiaxed micrograins (Fig. 5(d) and (e)). The process of transformation from Fig. 5(d) to 5(e) needs a diffusional reorientation of small segments of grain boundaries. The time required for this reorientation (of approximately 0.5 rad at the temperature of $0.5T_m$) has been calculated for different grain sizes. For 0.1 μm, they obtained times consistent with the deformation times (on the order of fraction of milliseconds). The result of such a calculation for copper is shown in Figure 6. It is concluded that a rotational mechanism, accompanied by grain-boundary reorientations can account for the structures observed. It is by no means claimed this is the only mechanism operating in shear localization. Nevertheless it is an important one, and explains the nanocrystalline structures observed.

3. Self-organization

Shear bands constitute the primary carriers of inelastic strain in high strain-rate deformation. In a manner analogous to dislocations, that are the primary carriers of plastic deformation in metals, the shear bands organize themselves with specific governing relations that are not fully understood yet. Their spacing is dependent on a number of material and loading parameters. Examples of these parameters are the number and potency of initiation sites, velocity of propagation, externally applied strain rate, and stress state.

Three possible mechanisms for the spacing of shear bands have been proposed:

(i) the Grady–Kipp momentum diffusion mechanism;

(ii) the Wright–Ockendon–Molinari perturbation mechanism; and

(iii) a mechanism based on microstructural inhomogeneities.

Grady and Kipp (1987) proposed that the rapid loss of strength across the developing shear band affects neighboring material by forcing it to unload. This theory is actually an extension of the Mott (1947) fragmentation model to the shear configuration. This process of unloading is communicated outward by momentum diffusion, rather than by elastic wave propagation. Figure 7(a) shows a shear band (thickness a) with the displacement fields at two times t_1 and t_2. At t_1 the displacement is zero. A shielded region propagates away from the band. It is represented by the rigid-plastic interface in Figure 7(a). The minimum separation between independently nucleating

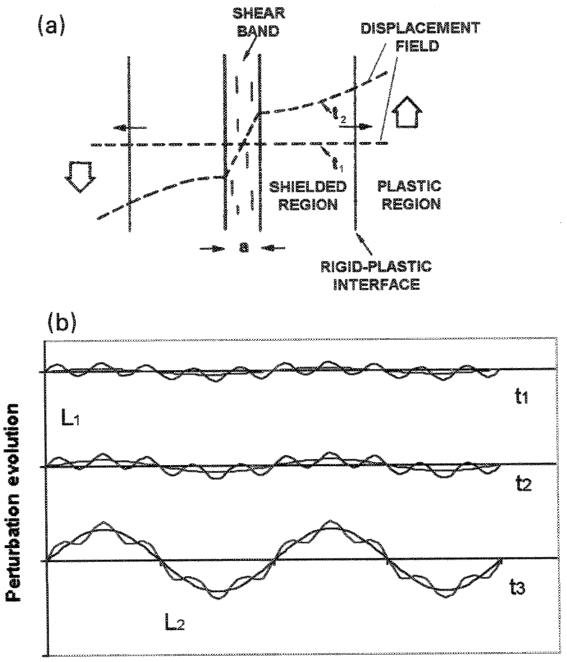

Figure 7
Two mechanisms of determining shear band spacing (a) momentum diffusion (after Grady and Kipp 1987) and (b) growth of perturbation t successive times t_1, t_2, and t_3.

bands arises from computing the distance traveled by the diffusive unloading front during the time required to unload as localization occurs. The predicted spacing, L_{GK} is:

$$L_{GK} = 2\left[\frac{9k_1C}{\dot{\gamma}_0^3 a^2 \tau_0}\right]^{1/4} \tag{6}$$

In Eqn. (6) the applied shear strain rate is $\dot{\gamma}_0$, and the flow stress is assumed to be a linear function of temperature with a softening coefficient, a, (T_r is a reference temperature, at which the flow stress is equal to τ_0):

$$\tau = \tau_0[1 - a(T - T_r)] \tag{7}$$

Grady and Kipp (1987) considered a simple rate-independent material.

Wright and Ockendon (1996) developed an analysis based on the notion that shear bands arise from small growing disturbances in an otherwise uniform region. This concept had been previously advanced by Grady (1980). Disturbances do not propagate in perpendicular directions, but simply grow in place. Figure 7(b) shows, in schematic fashion, two wave trains at successive times, t_1, t_2, and t_3. The wave with the

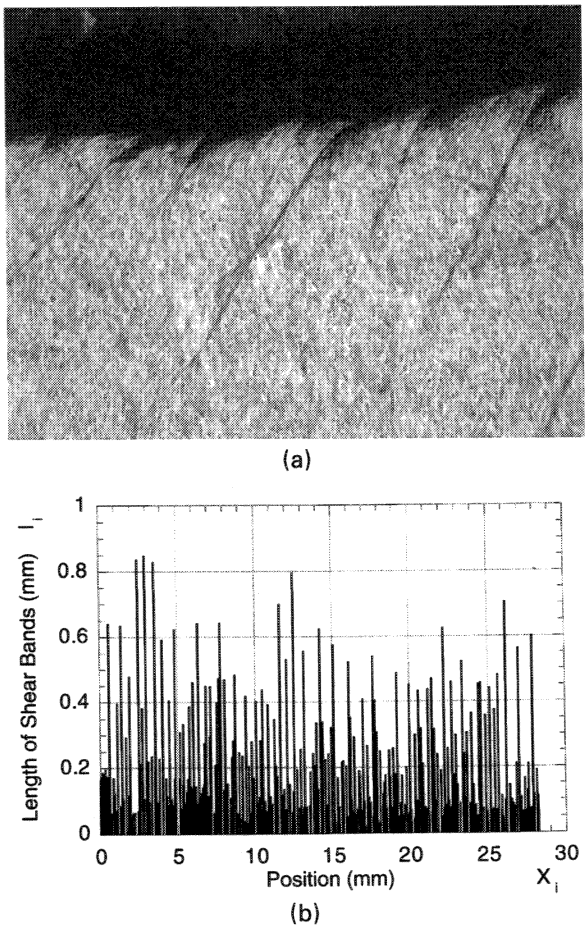

Figure 8
(a) Multiple shear bands produced in cylinder implosion test; shear bands initiated at internal surface (top of micrograph) due to higher local stresses, (b) Shear band spacing measured after 304 SS cylinder underwent global effective strain of 0.54 (from Shock Compression of Condensed Matter, 2000, pp. 431–34)

largest wavelength, L_2, shows a higher rate of amplitude increase. Thus, it gradually dominates the other wavelength, and will determine the spacing of the shear bands. The most likely minimum spacing is obtained by finding the fastest growing wavelength. Wright and Ockendon (1996) applied the perturbation analysis to the conservation equations according to the approach introduced by Clifton (1979) .The three equations and obtained a spacing, L_{WO}, equal to:

$$L_{WO} = 2\pi\left[\frac{m^3 k_1 C}{\dot{\gamma}_0^3 a^2 \tau_0}\right]^{1/4} \tag{8}$$

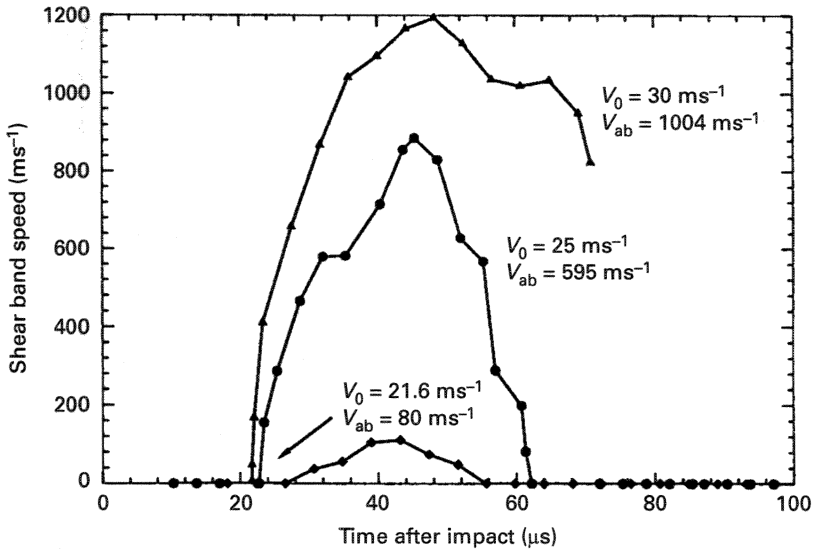

Figure 9
Velocity of propagation of shear-band tip in C-300 steel (from *J. Mech. Phys. Sol.*, 1997, 1007)

The material flow stress was assumed to be both temperature and strain-rate dependent; hence Eqn. (8) was modified by incorporating strain rate effects through parameter m ($\dot{\gamma}_0$ is a reference strain rate):

$$\tau = \tau_0[1 - a(T - T_0)]\left(\frac{\dot{\gamma}}{\dot{\gamma}_0}\right)^m \tag{9}$$

Although the approaches taken by Grady and Kipp and by Wright and Ockendon are completely different—the former concentrating on the stress collapse mechanism, and the latter concentrating on the earliest stages of localization—it is a remarkable fact that except for numerical factors and the rate constants, the two results are the same. The major difference between Eqns. (6) and (8) is that strain rate sensitivity affects the spacing in Wright–Ockendon model and is not present in the Grady–Kipp model.

Molinari (1997) further developed the analysis; in this model the important step which determines the shear band spacing is related to the early stages of flow localization, as in the Wright–Ockendon model. The important feature of Molinari's model is that it includes the strain-hardening effect; the nonstrain-hardening case can be obtained as a special case. For power law strain hardening, Molinari (1997) obtained the spacing, given by:

$$L_M = \frac{2\pi}{\xi_0}\left(1 + \frac{3}{4}\frac{\rho C \dfrac{\partial \dot{\gamma}}{\partial \gamma}}{\beta \tau_0 \dfrac{\partial \dot{\gamma}}{\partial T}}\right) \tag{10}$$

for a constitutive equation of the form:

$$\tau = \mu_0(\gamma + \gamma_i)^n \left(\frac{\dot{\gamma}}{\dot{\gamma}_o}\right)^m \left(\frac{T}{T_r}\right)^\nu \tag{11}$$

where γ_i is a pre-strain and ξ_0 is the wave number of the perturbation; ν, n, m, and μ_0 are the material parameters.

Nesterenko *et al.* (1998) and Xue *et al.* (2000) carried out experiments on titanium and AISI 304 stainless steel, in which the maximum strain was varied. Figure 8(a) shows a typical array of shear bands (in stainless steel) forming on the internal surface of a cylinder, while Fig. 8(b) shows the distribution of lengths and spacing of the shear bands after the specimen has undergone an effective global strain of 0.54. The shear bands have different lengths and the models presented above are only a first attempt at understanding the complex interactions. As the shear bands grow, they establish a different spacing pattern. The two-dimensional nature of the process cannot be ignored and the evolution of spacing cannot be accommodated by the one-dimensional Grady–Kipp, Wright–Ockendon, or Molinari approaches. It seems that the Wright–Ockendon–Molinari mechanism describes the initiation better, whereas Grady–Kipp represents the shear-band spacing at a well developed stage. Prior to the onset of localization, momentum diffusion is absent, and its role is only felt in the propagation stage. Local fluctuations in strain and temperature lead to the initiation.

It is important to connect the Wright–Ockendon–Molinari and Grady–Kipp models to microstructural processes happening in the material. It is even possible that microstructural inhomogeneities rather than

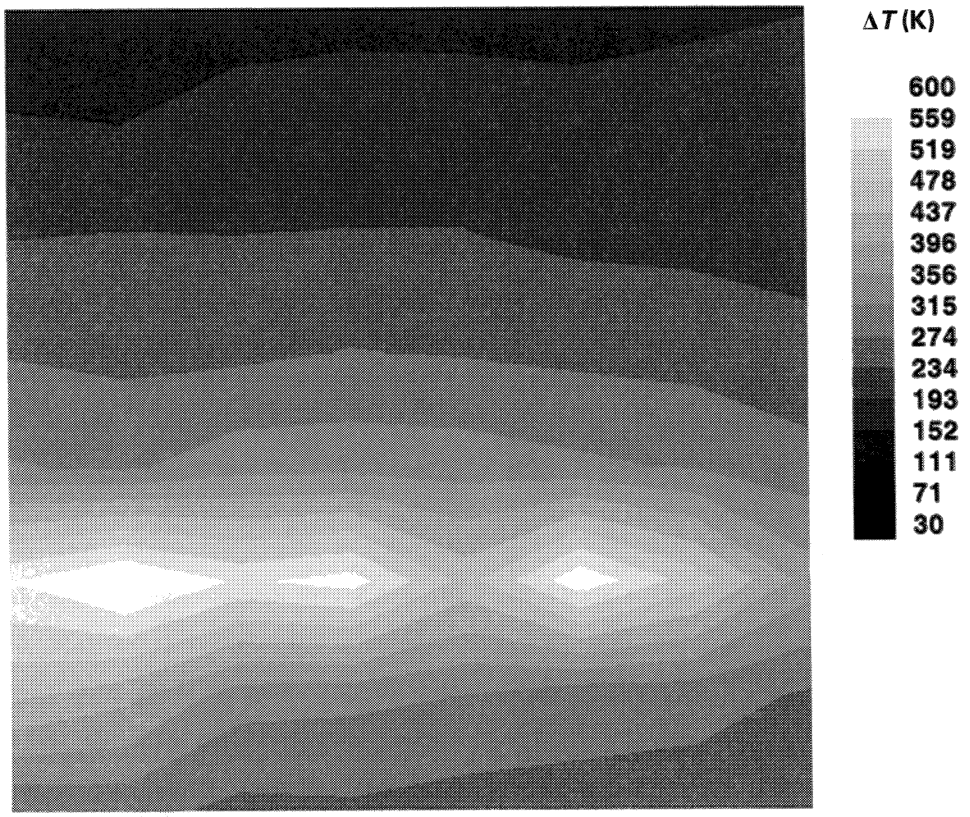

Figure 10
Temperature rise during propagation of a shear band in high strength martensitic C 300 steel (from SM Report 00–9, California Institute of Technology, 2000)

strain/temperature perturbations or momentum diffusion, are the determining factors in spacing. Possible micromechanisms for the initiation of shear bands have been discussed by Nesterenko *et al.* (1998).

In ceramics, shear bands were also observed and they also exhibit a characteristic spacing. As mentioned before, the softening is not produced by the thermal excursion. Two different softening mechanisms were observed:

(i) comminution of material within the shear zone, leading to a decreased overall need for dilatation; and

(ii) thermal softening of smaller particles, ductilizing the material.

There is a distinct difference between prefractured and granular material. Al_2O_3 (Chen *et al.* 1996, Nesterenko *et al.* 1996) and SiC (Shih *et al.* 1998) showed consistent shear band spacings: 0.4–1 mm for the granular condition and 1.7–3 mm for the prefractured condition. The reasons for these differences are still poorly understood and could be due to the softening rate. In the momentum diffusion formulation, the higher the unloading rate along a band, the lower the spacing among shear bands. Differences in initial density could also account for the greater shear-band spacing for the prefractured material: the density of the (precompacted) granular ceramic is only 85% of the theoretical value.

For metallic glasses and polymers, practically nothing is known about the self-organization of shear bands; the spacing seems to be around 0.6 mm.

4. *Velocity of Propagation, Temperature, and Vorticity*

Shear bands cannot be considered as a one-dimensional phenomenon. They are inherently two-dimensional, and are formed as a result of the propagation of the shear-band tip, as emphasized by Kuriyama and Meyers (1986). Freund *et al.* (1985) and Mercier and Molinari (1998) proposed models addressing the propagation velocity of a shear-band tip. Zhou *et al.* (1997) measured the velocity of propagation of shear bands in a martensitic C 300 steel and Ti-6%Al-4%V alloy. Characteristic results for steel

are shown in Fig. 9. The shear band accelerates to a characteristic velocity, which is a function of the external driving force. In the case of Zhou *et al.* (1997), the impact velocity was varied. The velocity can reach values approaching the shear-wave velocity. By increasing the impact velocity from $21.6\,m\,s^{-1}$ to $30\,m\,s^{-1}$, the shear-band propagation velocity in C 300 steel increased from $80\,m\,s^{-1}$ to $1000\,m\,s^{-1}$. In the titanium alloy, the measured velocities were much lower. These results illustrate the large range in the propagation velocities.

The temperatures within the shear bands can be calculated and measured. The first measurements are due to Duffy. As the infrared measurement systems evolve, the ability to determine the local temperature and its evolution is enhanced. The early systems averaged the temperature over larger areas (often considerably larger than the thickness of the bands). An example of an advanced measurement system consists of an 8×8 matrix of detectors that can acquire readings at 10^6 frames per second. A picture of the temperature distribution at a specific time, t, (all detectors are activated simultaneously) is shown in Fig. 9. The maximum increase is approximately 600 K. The periodic nature of temperature fluctuation is clearly seen. These pulsations were found to travel along the band, leading to the conclusion that vortical processes occurred at the shear band, confirming earlier predictions by Freund *et al.* (1985) and Mercier and Molinari (1998).

5. *Conclusions*

Shear localization is known to play an important role in the inelastic deformation of materials at high strain rates. The microstructural processes occurring in the different classes of materials are presented:

5.1 Metals

Thermal softening is the first stage of this process, leading to a number of softening processes including dynamic recovery and recrystallization, precipitate dissolution, phase transformations, melting and amorphization, crystallization (in metallic glasses).

5.2 Ceramics and Rocks

Granular and prefractured ceramic (Al_2O_3 and SiC) were analyzed and shear localization was found to occur by two different mechanisms, dependent upon particle size: particle break-up/comminution, when the size exceeds a critical value, a_c, or particle repacking and plastic deformation with significant heat evolution leading, under extreme conditions, to resintering of particles when the size is below the critical value, a_c.

5.3 Noncrystalline Metals and Polymers

The deformation processes leading to large-scale localization are most probably initiated by "local inelastic shear transformation zones" (Argon 1999) that form in a cooperative manner and organize themselves into shear zones, or by Volterra dislocation loops organizing themselves into sheared areas (Somigliana dislocations) as postulated by Li (see *Plastic Deformation of Noncrystalline Materials*).

Acknowledgment

This work was funded by the US Army Research Office.

Bibliography

Anand L, Kalidindi S R 1994 *Mech. Mater.* **17**, 223
Andrade U R, Meyers M A, Chokshi A H 1994 *Scr. Metall. Mater.* **30**, 933
Argon A S 1999 Rate processes in plastic deformation of crystalline and noncrystalline solids. In: Meyers M A, Armstrong R R, Kirchner H O K (eds.) *Mechanics and Materials*. Wiley, New York, Chap. 7
Armstrong R W, Batra R, Meyers M A, Wright T W 1994 *Mech. Mater.* **12**, 83–328
Armstrong R W, Coffey C S, Elban W L 1982 *Acta Met.* **30**, 2111
Bai Y 1981 In: Meyers M A, Murr L E (eds.) *Shock Waves and High Strain-rate Phenomena in Metals: Concepts and Applications*. Plenum, New York, p. 277
Chen H C, Meyers M A, Nesterenko V F 1996 In: Schmidt S C, Tao W C (eds.) *Shock Compression of Condensed Matter*. AIP Press, pp. 607
Clifton R J 1979 *Material Response to Ultra-high Loading Rates*. NMAB, NAS, Washington, DC, Rep. NMAB-356, Chap. 8
Derby B 1991 *Acta Metall.* **39**, 955
Fressengeas C, Molinari A 1987 *J. Mech. Phys. Sol.* **35**, 185
Freund L B, Wu F H, Toulios M 1985 *Proc. Symp. Considere Memorial*. Presse de l'Ecoles Nationale des Ponts et Chaussees, Paris, France
Grady D E 1980 *J. Geophys. Res.* **85**, 913
Grady D E 1994 *Mech. Mater.* **17**, 289
Grady D E, Kipp M E 1987 *J. Mech. Phys. Solid*, **35**, 95
Grebe H A, Pak H R, Meyers M A 1985 *Metall. Trans.* **16A**, 711
Kuriyama S, Meyers M A 1986 *Metall. Trans.* AlA., 443
Le Roy Y M, Molinari A 1993 *J. Mech. Phys. Sol.* **41**, 631
Mercier S, Molinari A 1998 *J. Mech. Phys. Sol.* **46**, 1463–95
Meunier Y, Roux R, Moureaud J 1992 In: *Shock Wave and High Strain-rate Phenomena in Materials*. Dekker, New York, pp. 637
Meyers M A 1994 *Dynamic Behavior of Materials*. Wiley, New York
Meyers M A, Chen Y J, Marquis F D S, Kim D S 1995 *Metall. Mater. Trans.* **26A**, 2493
Meyers M A, Hsu K C, Couch-Robino K 1983 *Mater. Sci. Eng.* **59**, 235
Meyers M A, Pak H R 1986 *Acta Metall.* **34**, 2493
Meyers M A, Subhash G, Kad B K, Prasad L 1994 *Mech. Mater.* **17**, 175
Meyers M A, Wittman C L 1990 *Metall. Trans.* **21A**, 3193

Molinari A 1997 *J. Mech. Phys. Sol.* **45**, 1551
Molinari A, Clifton R J 1983 *Comptes Rendus* **296**, 1
Molinari A, Le Roy Y M 1991 *Comptes Rendus* **313**, 7
Mott N F 1947 *Proc. R. Soc. London A* **189**, 300
Nesterenko V F, Meyers M A, Chen H C 1996 *Acta Metall.* **44**, 2017
Nesterenko V F, Meyers M A, Chen H C, LaSalvia J C 1994 *Appl. Phys. Lett.* **65**, 3069–71
Nesterenko V F, Meyers M A, LaSalvia J C, Bondar M P, Chen Y J, Lukyanov Y L 1997 *Mater. Sci. Eng. A* **229**, 23
Nesterenko V F, Meyers M A, Wright T W 1998 *Acta Mater.* **46**, 327–40
Nesterenko V F, Xue Q, Meyers M A, Wright T W 1999 In: Khan A S (ed.) *Proc. 7th Int. Symp. Plasticity and its Current Applications: Plasticity '99*. Neat Press, pp. 507
Olson G B, Mescall J F, Azrin M 1981 In: Meyers M A, Murr L E (eds.) *Shock Waves and High Strain-rate Phenomena in Metals*. Plenum, New York, pp. 221–47
Peirce D, Asaro R J, Needleman A 1984 *Acta Metall.* **31**, 1951
Recht R F 1964 *J. Appl. Mech.* **31**, 189
Rogers H C 1979 *Annu. Rev. Mater. Sci.* **2**, 283
Rudinicki J W, Rice J R 1975 *J. Mech. Phys. Sol.* **23**, 371
Shih C J, Meyers M A, Nesterenko V F 1998 *Acta Mater.* **11**, 4037
Shih C J, Nesterenko V F, Meyers M A 1998 *J. Appl. Phys.* **83**, 4660
Stelly M, Dormeval R 1986 In: Murr L E, Staudhammer K P, Meyers M A (eds.) *Metallurgical Applications of Shock Wave and High Strain-rate Phenomena*. Dekker, New York, p. 607
Stelly M, Legrand J, Dormeval R 1981 In: Meyers M A, Murr L E (eds.) *Shock Waves and High Strain-rate Phenomena in Metals*. Plenum, New York, pp. 113–25
Weertman J, Hecker S S 1983 *Mech. Mater.* **2**, 89
Wittman C L, Meyers M A, Pak H R 1990 *Metall. Trans.* **21A**, 707
Wright T W, Ockendon H 1996 *Int. J. Plast.* **12**, 927
Xue Q, Bai Y, Shen L 1992 *Proc. 2nd Int. Symp. ISIDL*. Chengdu, China, pp. 405–8
Xue Q, Nesterenko V F, Meyers M A 2000 Self-organization of adiabatic shear bands in Ti, Ti-6Al-4V and stainless steel. In: (ed.) *Shock Compression of Condensed Matter*. AIP, pp. 431–4
Zener C, Holloman J H 1944 *J. Appl. Phys.* **15**, 22
Zhou M, Ravichandran G, Rosakis A 1997 *J. Mech. Phys. Sol.* **44**, 981–1007

M. A. Meyers

Encyclopedia of Materials: Science and Technology
ISBN: 0-08-0431526
pp. 7093–7103